

Ground-state structure of coherent lattice-mismatched zinc-blende $A_{1-x}B_xC$ semiconductor alloys ($x=0.25$ and 0.75)

Shiyu Chen and X. G. Gong

Surface Science Laboratory (National Key) and Physics Department, Fudan University, Shanghai 200433, People's Republic of China

Su-Huai Wei

National Renewable Energy Laboratory, Golden, Colorado 80401, USA

(Received 26 November 2007; published 15 February 2008)

Using valence force-field and first-principles total-energy calculations, we investigate the relative stability of possible ground-state structures, famatinite, Q8, and Q16, proposed in previous ground-state searches for coherent lattice-mismatched zinc-blende $A_{1-x}B_xC$ ($x=0.25$ and 0.75) semiconductor alloys. Our total-energy calculations show that among all the alloys, the Q8 or Q16 are the possible ground-state structures with the lowest total energies, whereas the famatinite structure is not. The observed trends are explained in terms of strain and the Coulomb energy contributions in these lattice-mismatched semiconductor alloys.

DOI: 10.1103/PhysRevB.77.073305

PACS number(s): 61.50.Ah, 61.66.Dk, 61.82.Fk

Physical properties of the semiconductor alloy $A_{1-x}B_xC$ can be tuned by its atomic configuration as well as the alloy concentration x . Therefore, understanding the alloy stability and physical properties as functions of the atomic configuration has attracted much attention in the last 20 years.^{1–10} For the lattice-mismatched zinc-blende semiconductor alloy, it has been shown that due to bond-length mismatch induced strain, the ground state at $T=0$ K is phase separated AC and BC zinc-blende compounds. However, under coherent strained condition (i.e., no bond-breaking phase separation), the freestanding lowest energy ground-state structures can have different configurations. Using cluster expansion and an exhaustive enumeration approach,¹¹ Ferreira *et al.* found that the coherent ground state at $x=0.5$ has the chalcopyrite (CH) structure, which can be described as an $(AC)_2(BC)_2$ layered structure along the $[201]$ direction.² They showed that the CH structure has the smallest bond angle distortion when the C atom is displaced to accommodate the mismatched $A-C$ and $B-C$ bond lengths; therefore, it has the minimum strain energy at $x=0.5$.^{2–4} Their observation has led to the prediction that under coherent strain condition, the metastable (with respect to the phase separation) chalcopyrite structure can form,^{2,4} which is consistent with experimental observations.¹² Their observations and predictions for the $x=0.5$ alloy were recently reconfirmed by Liu *et al.*⁸ using valence force field (VFF)^{13–15} and density functional¹⁶ for the total-energy calculations and the exhaustive enumeration approach¹¹ and the genetic algorithm method¹⁷ for the ground-state search of a group of lattice-mismatched III-V semiconductor alloys: GaInN, GaInP, GaInAs, GaInSb, InAsSb, and InPAs. However, for $Ga_{0.25}In_{0.75}N$, they predict that⁸ at $x=0.25$, the eight-atom unit-cell famatinite (FM) structure [Fig. 1(a)], which is an $(AC)_1(BC)_3$ layered structure along the $\langle 201 \rangle$ direction, has the lowest total energy, whereas in the previous ground-state search,² it has been shown that the ground state for lattice-mismatched zinc-blende semiconductor alloys has the Q8 structure [Fig. 1(b)], which is a 16-atom unit-cell $(AC)_1(BC)_2(AC)_1(BC)_4$ layered structure along the $\langle 201 \rangle$ direction. It has also been suggested that, in some cases, the Q16 structure [Fig. 1(c)], which has

a 32-atom tetragonal unit cell and cannot be expressed as a layered structure, can have slightly lower total energy than the Q8 structure.⁶

To clarify this issue, we have performed VFF and density function total-energy calculations for the lattice-mismatched III-V alloys: $Ga_{1-x}In_xN$, $Ga_{1-x}In_xP$, $Ga_{1-x}In_xAs$, $GaN_{1-x}P_x$, $GaAs_{1-x}Sb_x$, and $InAs_{1-x}Sb_x$. We find that for all the systems studied here, the Q8 structure always has lower *total* energy than the FM structure at $x=0.25$ and 0.75 , and depending on the alloys, the Q16 structure, in some case, can have slightly lower total energy than that of the Q8 structure. This is

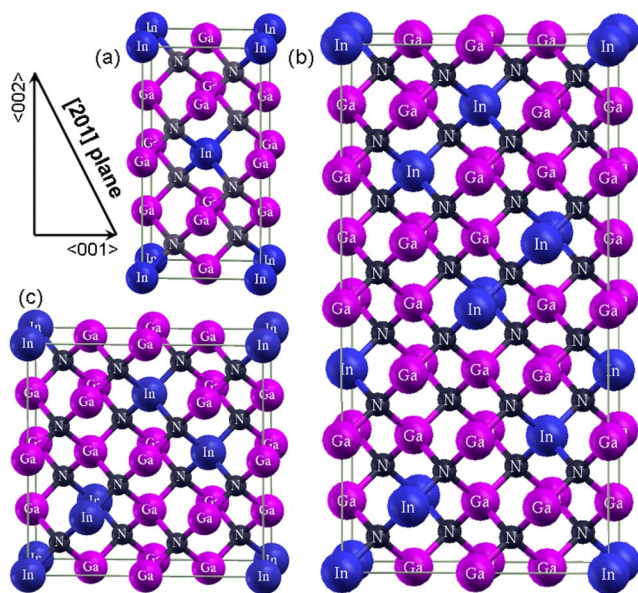


FIG. 1. (Color online) Atomic configuration of $Ga_{0.25}In_{0.75}N$ with (a) famatinite structure with lattice vectors $\vec{a}_1=\langle 1,0,0 \rangle$, $\vec{a}_2=\langle 0,1,0 \rangle$, and $\vec{a}_3=\langle 0.5,0.5,1 \rangle$, (b) Q8 structure with $\vec{a}_1=\langle 2,0,0 \rangle$, $\vec{a}_2=\langle 0,1,0 \rangle$, and $\vec{a}_3=\langle 1.5,0.5,1 \rangle$, and (c) Q16 structure with $\vec{a}_1=\langle 2,0,0 \rangle$, $\vec{a}_2=\langle 0,1,0 \rangle$, and $\vec{a}_3=\langle 0,0,2 \rangle$.

because for these semiconductor alloys, the Q8 and Q16 structures have less bond bending when the C atoms are displaced to accommodate the bond-length mismatch between AC and BC constituents and also because the Q8 and Q16 structures have lower Coulomb energy than the FM structure.⁵ Our results confirmed the previous predictions^{2,6} that the Q8 structure is more stable than the FM structure and therefore is the possible ground-state structure of lattice-mismatched $A_{1-x}B_xC$ alloys at $x=0.25$ and 0.75 . Structures with a larger unit cell could have lower total energy than the Q8 structure, but their total energy should be almost degenerate with the Q8 structure. In the following, we will describe in more detail our calculation methods and discuss our calculated results.

The formation enthalpy of $A_{1-x}B_xC$ alloy is defined as

$$\Delta H(x) = E(A_{1-x}B_xC) - [(1-x)E(AC) + xE(BC)], \quad (1)$$

in which $E(A_{1-x}B_xC)$, $E(AC)$, and $E(BC)$ are the total energies of the alloy $A_{1-x}B_xC$ and constituents AC and BC at their own equilibrium lattice constants, respectively. In this study, the total energies are calculated within the density functional formalism as implemented in the plane wave VASP code.^{16,18} For the exchange-correlation potential, we use the generalized gradient approximation (GGA) of Perdew and Wang, known as PW91.¹⁹ The Ga $3d$ and In $4d$ electrons are treated explicitly as valence electrons. The interaction between the core electrons and the valence electrons is included by the standard frozen-core projector augmented-wave potentials provided within the VASP package.^{20,21} An energy cutoff of 300 eV was applied in all cases. For the Brillouin-zone integration, we used the k -point meshes that are equivalent²² to the $6 \times 6 \times 6$ Monkhorst-Pack meshes²³ for an eight-atom cubic unit cell. All the lattice vectors and atomic positions are fully relaxed by minimizing the quantum mechanical stresses and forces.

It has been shown that for lattice-mismatched isovalent semiconductor alloys, the major contribution to the formation enthalpy is the strain energy, which, for conventional (with moderate lattice-mismatch) semiconductor alloys, can be described well by the VFF model.^{13–15} In this VFF model, the strain energy for configuration σ is given by

$$\Delta E_{VFF}(\sigma) = \sum_l \sum_{m=1}^4 \frac{3\alpha_{lm}}{8d_{lm}^2} [r_{lm}^2 - d_{lm}^2]^2 + \sum_l \sum_{s=1}^2 \sum_{k=1}^6 \frac{3\beta_{lsk}}{8d_{lsk1}d_{lsk2}} \times [r_{lsk1}r_{lsk2} \cos(\theta_{lsk}) - d_{lsk1}d_{lsk2} \cos(\theta_0)]^2, \quad (2)$$

in which l runs through all the fcc lattice sites in the unit cell, $s=1,2$ denotes the two sublattice sites in the zinc-blende cell, m runs through the four different bonds, and k runs through the six angles with the vertex at site ls . $lsk1$ and $lsk2$ represent the two bonds that form the angle k at the site ls . d_{lm} (similarly for d_{lsk1} and d_{lsk2}) is the ideal bond length for bond lm , whereas r_{lm} (similarly for r_{lsk1} and r_{lsk2}) is the corresponding calculated bond length. θ_{lsk} is the angle formed between bonds $lsk1$ and $lsk2$ and $\theta_0=109.5^\circ$ is the ideal tetrahedral bond angle. The first term on the right-hand side in Eq. (2) is the bond-stretching contribution to the strain energy originating from the bond-length deviations from the ideal bond lengths, while the second term is the bond-

TABLE I. Input parameters for VFF calculation from Refs. 15, 24, and 25, including the cation-anion distances d and force constants α and β for pure compounds.

Compound	d (Å)	α (N/m)	β (N/m)
GaN	1.9486	96.30	14.80
InN	2.1564	79.20	7.10
GaP	2.3612	47.32	10.46
InP	2.5495	43.04	6.24
GaAs	2.4480	41.19	8.94
InAs	2.6233	35.18	5.49
GaSb	2.6396	33.16	7.23
InSb	2.8057	26.61	4.28

bending contribution originating from the bond-angle deviations from the ideal tetrahedral angle. The ideal bond lengths d , bond-stretching elastic constants α , and bond-bending elastic constants β used in this study are listed in Table I.^{15,24,25} For the bond angle between mixed bonds $lsk1$ and $lsk2$, we use $\beta_{lsk} = (\beta_{lsk1} + \beta_{lsk2})/2$. We want to point out that the elastic constants are fitted to experimental data near the equilibrium; thus, when the alloy lattice constants differ significantly from the one for the binary constituent, errors due to the neglect of volume and bond-length dependence of the elastic constants are expected. In the following, we will first discuss our VFF-calculated results.

The strain energies calculated using the VFF functional [Eq. (2)] for $\text{Ga}_{1-x}\text{In}_x\text{N}$, $\text{Ga}_{1-x}\text{In}_x\text{P}$, $\text{Ga}_{1-x}\text{In}_x\text{As}$, $\text{Ga}_{1-x}\text{P}_x$, $\text{GaAs}_{1-x}\text{Sb}_x$, and $\text{InAs}_{1-x}\text{Sb}_x$ ($x=0.25$ and 0.75) alloys with FM, Q8, and Q16 structures (Fig. 1) are listed in Table II. We find that (i) the strain energies for Q8 and Q16 are very similar; the difference is usually less than 1 meV/atom. This

TABLE II. VFF-calculated strain energy $\Delta E_{VFF}(\sigma)$ (in meV/atom) of $\text{Ga}_{1-x}\text{In}_x\text{N}$, $\text{Ga}_{1-x}\text{In}_x\text{P}$, $\text{Ga}_{1-x}\text{In}_x\text{As}$, $\text{Ga}_{1-x}\text{P}_x$, $\text{GaAs}_{1-x}\text{Sb}_x$, and $\text{InAs}_{1-x}\text{Sb}_x$ alloys for the FM, Q8, and Q16 structures at $x=0.25$ and 0.75 .

Structures	FM	Q8	Q16
$\text{Ga}_{0.75}\text{In}_{0.25}\text{N}$	27.58	23.90	23.65
$\text{Ga}_{0.25}\text{In}_{0.75}\text{N}$	16.53	16.80	17.33
$\text{Ga}_{0.75}\text{In}_{0.25}\text{P}$	15.25	13.55	13.50
$\text{Ga}_{0.25}\text{In}_{0.75}\text{P}$	10.90	10.78	11.00
$\text{Ga}_{0.75}\text{In}_{0.25}\text{As}$	11.24	10.05	10.01
$\text{Ga}_{0.25}\text{In}_{0.75}\text{As}$	8.26	8.14	8.29
$\text{Ga}_{0.75}\text{P}_{0.25}$	104.97	92.41	91.95
$\text{Ga}_{0.25}\text{P}_{0.75}$	80.36	80.72	82.17
$\text{GaAs}_{0.75}\text{Sb}_{0.25}$	13.70	12.46	12.45
$\text{GaAs}_{0.25}\text{Sb}_{0.75}$	11.85	11.45	11.58
$\text{InAs}_{0.75}\text{Sb}_{0.25}$	8.03	7.28	7.29
$\text{InAs}_{0.25}\text{Sb}_{0.75}$	6.73	6.54	6.64

TABLE III. Atomic correlation functions $\Pi_{2,m}$ of m th nearest neighbor pair figures in the FM, Q8, and Q16 structures.

Structures	Π_0	$\Pi_{2,1}$	$\Pi_{2,2}$	$\Pi_{2,3}$	$\Pi_{2,4}$	$\Pi_{2,5}$	$\Pi_{2,6}$	$\Pi_{2,7}$	$\Pi_{2,8}$
FM	1	0	2/3	1/3	1/3	0	0	1	0
Q8	1	1/12	1/3	5/12	0	1/6	0	1	1
Q16	1	1/12	1/3	5/12	0	1/12	0	5/12	1/12

is not surprising because these two structures differ in their atomic pair correlation functions (see Table III) only starting at the fifth neighbor.⁶ (ii) The strain energy for $A_{0.75}B_{0.25}C$ is always larger than for $A_{0.25}B_{0.75}C$ (here, we use the convention that the ideal bond lengths $d_{BC} > d_{AC}$), indicating that the strain energy is asymmetric and it is more difficult to mix a larger atom into a smaller size compound than mix a smaller atom into a larger size compound. (iii) For $A_{0.75}B_{0.25}C$, the Q8 structure is always lower in energy than the FM structure. The difference could be quite large for systems with large size mismatch, such as $\text{Ga}_{0.75}\text{In}_{0.25}\text{N}$ and $\text{GaN}_{0.75}\text{P}_{0.25}$. Compared to the bond-stretching contribution, the bond-bending term contributes more to the lowering of the strain energy of the Q8 relative to FM structures, indicating that the Q8 structure can better accommodate the bond distance mismatch with smaller bond angle distortions. This is also consistent with the fact that the Q8 and Q16 structures have smaller $\Pi_{2,4}$ atomic correlation functions than the FM structure.² (iv) Similar trends also exist for $A_{0.25}B_{0.75}C$. However, the energy difference becomes much smaller. For $\text{Ga}_{0.25}\text{In}_{0.75}\text{N}$ and $\text{GaN}_{0.25}\text{P}_{0.75}$, the FM structure even has a slightly smaller VFF strain energy than the Q8 structure. However, we notice that the order of the stability is quite sensitive to the bond-bending elastic constant β . For example, if we change the β value for InN from 7.10 to 9.00 N/m, as one would expect when the volume of a compound is compressed, the strain energy of the FM structure will be higher than the Q8 structure for $\text{Ga}_{0.25}\text{In}_{0.75}\text{N}$.

Although the VFF model gives a generally correct trend of the relative stability of the alloy as a function of the configuration, it does not fully take into account the charge disparity between the mixed atoms and the nonharmonic effect in the elastic energy. The introduced error could be large when the chemical and size mismatches between AC and BC are large. To obtain a more accurate description of the stability of the alloys, in the following, we describe our results from first-principles total-energy calculations, in which no parameters are fitted to the zinc-blende constituents.

The GGA-calculated results are shown in Table IV. We find that the trend of the stability agrees quite well with the VFF calculation. The GGA results show that the FM structure is always higher in energy than the Q8 structure. This is true even for $\text{Ga}_{0.25}\text{In}_{0.75}\text{N}$ and $\text{GaN}_{0.25}\text{P}_{0.75}$, where the VFF model predicts that the FM structure has slightly lower strain energy than the Q8 structure. The reason for this reverse of the stability is that in first-principles GGA calculation, first, the elastic constants for AC and BC compounds are renormalized, becoming closer to each other in the alloy and thus

TABLE IV. GGA calculated formation enthalpies $\Delta H(x)$ (in meV/atom) of $\text{Ga}_{1-x}\text{In}_x\text{N}$, $\text{Ga}_{1-x}\text{In}_x\text{P}$, $\text{Ga}_{1-x}\text{In}_x\text{As}$, $\text{GaN}_{1-x}\text{P}_x$, $\text{GaAs}_{1-x}\text{Sb}_x$, and $\text{InAs}_{1-x}\text{Sb}_x$ alloys for the FM, Q8, and Q16 structures at $x=0.25$ and 0.75 . The numbers with a “*” indicate the ground-state formation enthalpies.

Structures	FM	Q8	Q16
$\text{Ga}_{0.75}\text{In}_{0.25}\text{N}$	25.23	19.05*	19.20
$\text{Ga}_{0.25}\text{In}_{0.75}\text{N}$	15.50	15.23*	16.32
$\text{Ga}_{0.75}\text{In}_{0.25}\text{P}$	13.54	10.70	10.51*
$\text{Ga}_{0.25}\text{In}_{0.75}\text{P}$	10.36	9.44*	9.57
$\text{Ga}_{0.75}\text{In}_{0.25}\text{As}$	10.50	8.10	7.88*
$\text{Ga}_{0.25}\text{In}_{0.75}\text{As}$	7.92	7.07*	7.12
$\text{GaN}_{0.75}\text{P}_{0.25}$	161.32	134.33*	135.26
$\text{GaN}_{0.25}\text{P}_{0.75}$	97.01	88.03*	88.62
$\text{GaAs}_{0.75}\text{Sb}_{0.25}$	16.71	13.28	13.02*
$\text{GaAs}_{0.25}\text{Sb}_{0.75}$	13.41	11.24	11.06*
$\text{InAs}_{0.75}\text{Sb}_{0.25}$	11.36	8.95	8.72*
$\text{InAs}_{0.25}\text{Sb}_{0.75}$	9.28	7.64	7.49*

reducing the disparity between the AC and BC compounds. Second, the Coulomb interaction resulting from the charge disparity between A and B atoms in the $A_{1-x}B_xC$ alloy is taken into account in the GGA calculations. As shown in Ref. 5, the Madelung constants of this interaction for the FM, Q8, and Q16 structures are 2.5257, 2.5614, and 2.5615, respectively, so the Madelung energy of the Q8 or Q16 structure is lower than that of FM, which stabilizes the Q8 and Q16 structures.

In conclusion, using first-principles total-energy calculations, we have shown that the Q8 structure, which is an $(AC)_1(BC)_2(AC)_1(BC)_4$ layered structure along the $\langle 201 \rangle$ direction, always has a lower total energy than the farnitine structure and, therefore, is the possible ground-state structure for coherent lattice-mismatched zinc-blende $A_{1-x}B_xC$ ($x=0.25$ and 0.75) semiconductor alloys. In some cases, the tetragonal Q16 structure, which is not a layered structure, may have a lower energy than the Q8 structure. However, in these cases, the two structures are almost degenerate in energy (with energy differences of less than 0.5 meV/atom). The relative stability of these structures is explained in terms of their different strain and Coulomb energy contributions and is in agreement with previous predictions.^{2,6} Experimental test of our predictions is called for.

The work at Fudan University is partially supported by the National Science Foundation of China, the Special Funds for Major State Basic Research, and the Shanghai Project. The computation is performed in the Supercomputer Center of Shanghai, the Supercomputer Center of Fudan University, and CCS. The work at NREL is funded by the U.S. Department of Energy under Contract No. DE-AC36-99GO10337.

- ¹A.-B. Chen and A. Sher, *Semiconductor Alloys: Physics and Materials Engineering* (Plenum, New York, 1995).
- ²S.-H. Wei, L. G. Ferreira, and A. Zunger, Phys. Rev. B **41**, 8240 (1990).
- ³J. E. Bernard, L. G. Ferreira, S.-H. Wei, and A. Zunger, Phys. Rev. B **38**, 6338 (1988).
- ⁴L. G. Ferreira, S.-H. Wei, and A. Zunger, Phys. Rev. B **40**, 3197 (1989).
- ⁵R. Magri, S.-H. Wei, and A. Zunger, Phys. Rev. B **42**, 11388 (1990).
- ⁶Z. W. Lu, D. B. Laks, S.-H. Wei, and A. Zunger, Phys. Rev. B **50**, 6642 (1994).
- ⁷L. K. Teles, L. G. Ferreira, L. M. R. Scolfaro, and J. R. Leite, Phys. Rev. B **69**, 245317 (2004).
- ⁸J. Z. Liu, G. Trimarchi, and A. Zunger, Phys. Rev. Lett. **99**, 145501 (2007).
- ⁹S.-H. Wei and A. Zunger, Phys. Rev. B **49**, 14337 (1994).
- ¹⁰S.-H. Wei and A. Zunger, Phys. Rev. B **57**, 8983 (1998).
- ¹¹L. G. Ferreira, S.-H. Wei, and A. Zunger, Int. J. Supercomput. Appl. **5**, 34 (1991).
- ¹²H. R. Jen, M. J. Cherng, and G. B. Stringfellow, Appl. Phys. Lett. **48**, 1603 (1986).
- ¹³P. Keating, Phys. Rev. **145**, 637 (1966).
- ¹⁴R. Martin, Phys. Rev. B **1**, 4005 (1970).
- ¹⁵J. L. Martins and A. Zunger, Phys. Rev. B **30**, 6217 (1984).
- ¹⁶G. Kresse and J. Furthmuller, Comput. Mater. Sci. **6**, 15 (1996).
- ¹⁷G. Trimarchi, P. Graf, and A. Zunger, Phys. Rev. B **74**, 014204 (2006).
- ¹⁸G. Kresse and J. Furthmuller, Phys. Rev. B **54**, 11169 (1996).
- ¹⁹J. P. Perdew, J. A. Chevary, S.-H. Vosko, K. A. Jackson, M. R. Pederson, D. J. Singh, and C. Fiolhais, Phys. Rev. B **46**, 6671 (1992).
- ²⁰P. E. Blochl, Phys. Rev. B **50**, 17953 (1994).
- ²¹G. Kresse and D. Joubert, Phys. Rev. B **59**, 1758 (1999).
- ²²S. Froyen, Phys. Rev. B **39**, 3168 (1989).
- ²³H. J. Monkhorst and J. D. Pack, Phys. Rev. B **13**, 5188 (1976).
- ²⁴K. Kim, W. R. L. Lambrecht, and B. Segall, Phys. Rev. B **53**, 16310 (1996).
- ²⁵S.-H. Wei and A. Zunger, Phys. Rev. B **60**, 5404 (1999).